

BUILDING BOUNDARY EXTRACTION FROM HIGH RESOLUTION IMAGERY AND LIDAR DATA

Liang Cheng*, Jianya Gong, Xiaoling Chen, Peng Han

State Key Laboratory of Information Engineering in Surveying, Mapping and Remote Sensing,
Wuhan University, Wuhan, China - lcheng.geo@gmail.com,
-(jgong, cxl)@lmars.whu.edu.cn, -zb34xiaowu@163.com

KEY WORDS: Building boundary, High resolution image, Lidar data, Data integration

ABSTRACT:

Building boundary data are necessary for the real estate industry, 3D city models and many other applications. In this study, a novel approach integrated high resolution imagery and Lidar data is proposed for automatically obtaining building boundaries with precise geometric position and details. The high resolution images were used to directly extract the building boundaries with precise geometric position, our approach is focused on improving the correctness and completeness of the extracted boundaries by integrating Lidar data. The approach consists of four steps: Lidar data processing, building image generation, line segment extraction, and boundary segment selection. Firstly, the segmented building points need to be determined from raw Lidar data. Then, a building image is generated by processing an original image using a bounding rectangle and a buffer, which are derived from the segmented building points. Based on the building image and rough principal direction constraints, an algorithm is proposed to estimate the principal orientations of a building, which ensures the accuracy and robustness of the subsequent line segments extraction. Finally, an algorithm based on Lidar point density analysis and Kmeans clustering is proposed to identify accurate boundary segments from the extracted line segments dynamically. The experiment results demonstrated that the proposed approach determined building boundaries well.

1. INTRODUCTION

Building boundary data are necessary for the real estate industry, city planning, homeland security, flood management, and many other applications. The extraction of building boundary is also a crucial and difficult step toward generating city models. The automatic extraction of a building boundary from an image has been a research issue for decades; many related studies have been reported. McGlone and Shufelt (1994) extracted building boundaries by calculating vanishing points using the Gaussian Sphere technique to detect horizontal and vertical lines. Mohan and Nevatia (1989) described an approach based on perceptual grouping for detecting and describing 3D objects in complex images and applied the method to detect and describe complex buildings in aerial images. Xu, et.al., (2002) employed a Gabor filter to eliminate noisy edges, and then used a Normalized Central Contour Sequence Moment to select regular contours. A detailed review of techniques for the automatic extraction of buildings from aerial images was made by Mayer (1999). However, a difficult problem still exists in automated extraction of building boundaries because it is almost impossible to automatically distinguish building boundaries from other line segments in a high accuracy only based on aerial imagery. Moreover, a robust solution for boundary extraction is needed because too much complex information is contained in an image, especially for a very high resolution image.

Many studies also focused on boundary extraction by using Lidar point clouds. Weidner (1996) used the difference between DSM and DTM to determine the building outlines. Vosselman & Sander (2001) and Haala & Brenner (1999) used plan maps to support boundary extraction from Lidar points. Many related

papers have been published (Morgan and Habib, 2002; Rottensteiner and Briese, 2002; Overby, et.al., 2004; Vosselman and Kessels, 2005; Brenner, 2005). In general, it is hard to obtain a detailed and geometric precise boundary only using Lidar point clouds considering its low spatial resolution. To eliminate noise effects and get building boundaries with precise geometric position, some researchers used the minimum description length (MDL) method to regularize the ragged building boundaries (Weidner and Forstner, 1995; Suveg and Vosselman, 2004). Zhang et.al.(2006) used Douglas-Peucker algorithm to remove noise in a footprint, then adjusted the building footprints based on estimated dominant directions. Sampath and Shan (2007) performed building boundary tracing by modifying a convex hull formation algorithm, then implemented boundary regularization by a hierarchical least squares solution with perpendicularity constraints. However, regularization quality is also dependent on the point density of Lidar data; and limitation of Lidar data resolution and errors in filtering processes may cause obvious offset and artefacts in the final regularized building boundary (Sampath and Shan, 2007).

Although it is difficult to obtain building boundaries with precise geometric position using Lidar data, Lidar data is able to directly provide measured three-dimensional points. On the other hand, although very high resolution images can provide building boundaries with precise geometric position, the accuracy of automatic boundary extraction is still in a low level. It seems to be valuable to extract building boundaries by integrating very high resolution imagery and Lidar data. However, how to integrate the two data sources for building boundary extraction is still a problem; few approaches with technical details has been published (Rottensteiner, 2005).

* Corresponding author.

2. METHODS

In this study, a new approach integrating very high resolution imagery and Lidar data is proposed to automatically obtain detailed building boundaries with precise geometric position. The proposed approach can be proved to preserve the boundary details, including some tiny segments at a corner, a short segment. Since the boundaries with precise geometric position can be directly extracted from very high resolution images (e.g., 5cm spatial resolution); our approach is focused on improving the correctness and completeness of the extracted boundaries by integrating Lidar data. This process consists of four steps: Lidar data processing, building image generation, line segment extraction, and boundary segment selection. Firstly, the segmented building points need to be determined from raw Lidar data. Secondly, a building image is generated by a building bounding rectangle and a building buffer. Thirdly, a new algorithm is proposed for determining the principal orientations of building boundaries based on rough principal orientations constraint, which ensures the accuracy and robustness of the subsequent line segments extraction. Finally, an algorithm based on Lidar point density analysis and Kmeans clustering is proposed to provide a dynamic way to accurately identify boundary segments from non-boundary segments.

The proposed approach is focused on building boundary extraction and can be used in 3D building model reconstruction and 2D building digital line graph generation. Stereo aerial images should be selected for 3D building reconstruction and the extracted boundaries will be the basic elements of the subsequent processes such as line segments matching and 3D line segments generation. While an orthoimage would be more appropriate than an aerial stereo pair for getting a 2D digital line graph. Aerial stereo, orthoimage, or some other images can be processed by using a little different strategy of data registration as declared in the next section.

2.1 Data pre-processing (Lidar data processing)

In order to obtain the segmented building points from raw Lidar data, the first process is usually to separate the ground points from non-ground points, and then identify the building points from non-ground points. Numerous algorithms have been developed to separate ground points from non-ground points. Sithole and Vosselman (2004) made a comparative study of eight filters and identified that all filters perform well in smooth rural landscapes, but all of them produce errors in complex urban areas and rough terrain covered by vegetation. They also pointed out that the filters estimating local surfaces were found to perform best. So the linear prediction algorithm proposed by Kraus and Pfeifer (1998) is used for deriving bare DEM from raw Lidar data. Comparing the bare DEM and the raw Lidar data, non-ground points can be identified.

In a dataset that contains only non-ground points, building points need to be separated from non-building data (mainly vegetation). The region-growing algorithm based on a plane-fitting technique proposed by Zhang, et.al.(2006) is used. In this process, areas of non-ground points are firstly found and labelled by connecting the eight neighbours of a cell. For each non-ground area, inside and boundary points are identified. Then non-ground points for each area are segmented by region growing based on a plane-fitting technique. Finally, the segmented patches for non-building objects are removed. The remaining patches are identified as building patches. It is reported that the omission and commission errors of determined building are 10% and 2% respectively using this approach

2.2 Building image generation

In order to retrieve the interested building features from a very high resolution image, a building image is firstly generated to reduce the complexity of processes. In a building image, only one building is covered and non-building features are removed. A building image is generated by 3 steps as follows.

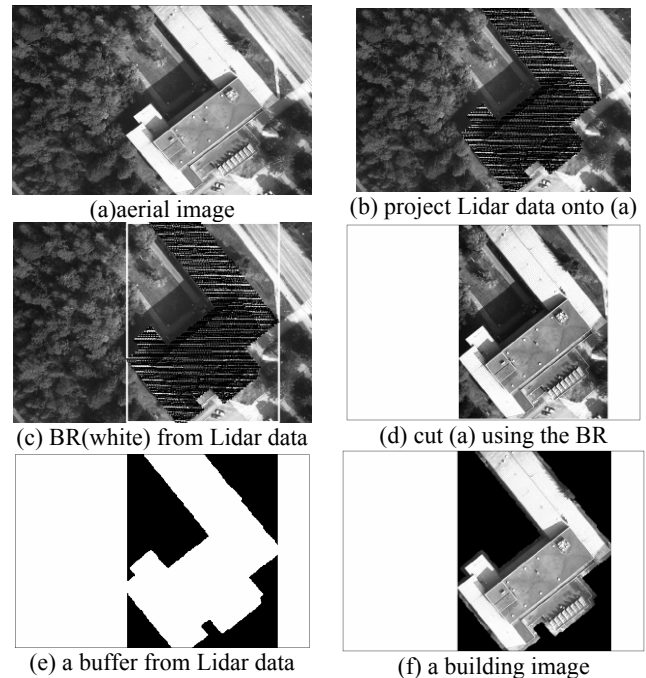


Figure 1. Steps of a building image generation

Step 1, Data overlay

In this step, images from different sensors can be processed using different strategies of data registration for different specific applications. An aerial stereo with orientation parameters is used in this study, Lidar points are directly projected onto the aerial stereo by collinearity equation. If necessary, the orientation parameters can be refined by block bundle adjustment. If an orthoimage is used, it can be directly overlain by Lidar data, as both spatial references are at the same coordinate system. For an image with unknown orientation parameters, the overlay between the image and Lidar data can be done by a manual co-registration operation. Figure 1 (a) is an oriented aerial image, Figure 1 (b) are the results by projecting the pre-processed Lidar data onto the aerial image using collinearity equation.

Step 2, Image cutting by a bounding rectangle (BR)

After a convex hull is constructed based on the projected Lidar points in 1 (b), a bounding rectangle (BR) of a building can be created based on the convex hull which is shown as a white rectangle on the image in 1 (c). The BR should be enlarged with a threshold to ensure all the boundaries of a building in the aerial image can be fully covered. The result cut from the aerial image in 1 (a) using the BR is shown in 1 (d).

Step 3, Image filtered by a buffering zone

A raster image is generated by interpolating the projected Lidar data in Figure 1 (b), and then a buffering image can be created shown in Figure 1(e). Figure 1(f) is the result by filtering the Figure 1(d) using the buffering zone, in which non-building features are removed from the image to get a building image.

As a building image is only generated for one building, the complexity of image processes is largely reduced. In the processes, thresholds are needed for creating a BR and a buffering zone determined based on the average point spacing of Lidar data, the spatial resolution of imagery and the accuracy of data registration. For a building image generation, the top-left coordinates of each building image need to be properly recorded, so that the line segments extracted from a building image can be correctly transformed onto the original image.

2.3 Line segments extraction

2.3.1 Principal orientation determination

Most of buildings are rectangular buildings, whose boundaries have perpendicular structures with two rectilinear axes. These two perpendicular axes have the most dominant contexture and can be treated as two major principal axes. The dominant orientations can be determined from the angle values statistics of the line segments. Rau and Chen (2003) proposed a straight line detecting method using Hough transform with principal axis analysis to speed up the extraction of straight lines and improve the accuracy of detecting lines, in which the key issue is to obtain the principal orientations of a building using Hough transformation in an image space before line segments extraction. A few limitations still exist in this method. One of the limits shows its sensitive to the principal orientations determination of a building in an image analysis. In this process, wrong principal orientations may be obtained, especially when poor or high repeatedly textures are appeared in the image. Another limit occurs at threshold selection, which is needed for filtering counting values in accumulative array from a Hough transformation to construct an angle-count histogram. The third limit is hard to process an image with complicated and irregular building layouts.

In this study, an algorithm is proposed for determining the principal orientations of a building. The principal orientations can be accurately and robustly determined based on the building image and rough principal orientations constraints. The building image is generated, and the rough principal orientations of a building can be obtained by analyzing the segmented building Lidar points. The proposed algorithm consists of two steps: rough principal orientation estimation and principal orientation determination.

(1) Rough principal orientation estimation

Based on the segmented building points, rough principal orientations of a building can be estimated by analyzing the Lidar points belonging to the building. A least square approach proposed by Chaudhuri and Samal (2007) is usually used to determine the directions of major and minor axes of discrete points. The method is used to determine the principal orientations of a building in this study. Considering the various geometric shapes of the buildings, a value range is constructed for a rough principal orientation by a threshold, which replaces the deterministic value of rough principal orientation in the following processes. In most cases, the threshold value is set as 5.

(2) Principal orientation determination

The principle directions are determined by finding maximum values in accumulative array from a Hough transformation which fall within estimated ranges of rough principle directions. There are only two principle directions for a building. Based on the rough principal orientation constraints, principal orientation determination consists of the following 7 steps.

Step a: Selecting a building image;

Step b: Applying Hough transformation on the image, and finding the maximum value M in the whole accumulative array;

Step c: Setting a threshold $T=M*t$ (the initial value of t is set to 0.9), and keeping those cells in accumulative array with value greater than the threshold T ;

Step d: Selecting the range of one rough principle direction;

Step e: Adding the counting numbers with the same θ value in the range. If all the accumulative values equal 0, then decreasing the value of t and going back to step c, if t is greater than 0; if t equals 0, the whole processing failed. If some accumulative values are greater than 0, go to next step;

Step f: Selecting the range of the other rough principle direction and go to step e. If both rough principle directions are processed, go to step g.

Step g: Detecting a peak in each of the two ranges. Each peak refers to a principal orientation of a building.

The advantages of the proposed algorithm are in three points. (1) Based on the building image, the principal orientation determination on any complicated building layouts can be easily decomposed into some sub-processes on each individual building, which make the principal orientation determination on any complex images become possible. (2) To get the principal orientations of an image, the peak detection just needs to be performed in the specific range of a histogram based on rough principal orientations constraint by the proposed algorithm, which can improve the robustness of the principal orientation determination. (3) The automation degree of principal orientations determination is also enhanced because the threshold of accumulative array can be determined in self-adaptive way.

2.3.2 Line segments extraction

Having compared the most existing edge detectors, Edison detector is chosen to perform edge detection. Then the line segments are extracted using Hough transformation with principal orientations constraint. The line segments extraction becomes accurate and robust, because peak detection in the accumulative array just needs to be performed on the principal orientations. Since the number of line segments in an image is unknown, it is necessary to specify conditions to terminate an algorithm. A dynamic termination condition usually works better than a static one. Adaptive Cluster Detection (ACD) algorithm is a classical dynamic method to detect straight lines based on Hough Transform. In this study, a modified ACD algorithm is proposed by setting the searching priority for peak detection according to the principal orientations; the other processes are same as ACD algorithm. The thresholds of the minimum length of line segment and of the minimum distance between line segments are 20 and 20, respectively. Based on the determined principal orientations, line segments extraction becomes more accurate and robust. A few line segments with weak signals (but always important) on principal orientation can be extracted robustly with the principal orientations constraint, which may be missed by traditional ACD algorithm because of ambiguity in peak detection. It avoids missing boundary details.

2.4 Boundary segments selection

In this section, the extracted line segments will be automatically separated into two sets: boundary segments and non-boundary segments. Although the principal orientations constraint is used during the line segments extraction, there still exist many non-boundary segments, especially the line segments of the building

rooftops which have the same directions as the boundaries. To remove the non-boundary segments, some solutions based on

Lidar data were proposed

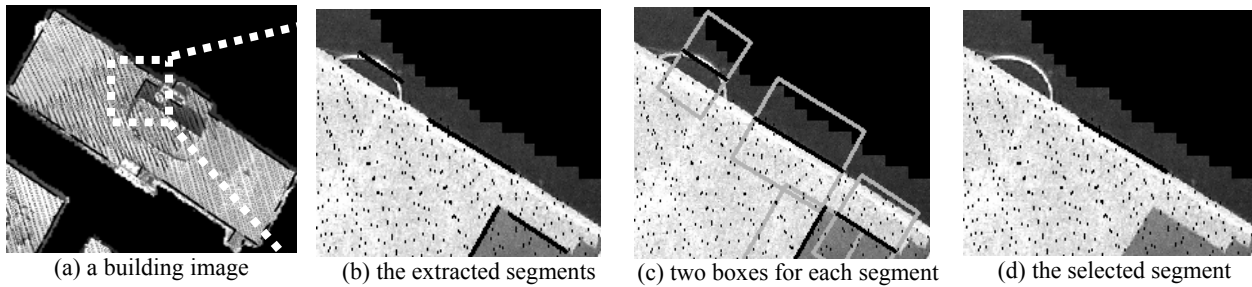


Figure 2. Accurate boundary segments selected by our algorithm

(Schenk & Csatho, 2002; Ma, 2004). The common idea of these solutions is to get approximate building boundaries from Lidar data, then remove the line segments far from the approximate boundaries. The limitations of these solutions are mainly in two points. Firstly, the quality of the approximate boundaries determined by Lidar data is uncertain, which is largely influenced by the quality of Lidar data filtering processing. Secondly, how to dynamically select the optimal boundaries in a local region is a problem. Sohn and Sampath (2003) proposed a different boundary filtering solution on IKONOS with Lidar data. However, compared to IKONOS, there exist much more possible object segments in a local region extracted from very high resolution imagery. In order to get an accurate boundary from a very high resolution image, a rigor selection rule should be used. An algorithm based on Lidar point density analysis and Kmeans clustering is proposed to ensure the accuracy of the selected boundary segments in a very high resolution image in this study. Figure 2(a) is a building image, the extracted line segments in a local region is shown in Figure 2(b). Based on the extracted line segments, the boundary segments selection algorithm consists of 4 steps as follows.

Step 1: Two rectangle boxes with a certain width (3-5 times Lidar points spacing) are generated along two orthogonal directions of a boundary segment. Two rectangle boxes are created for each segment, as shown in Figure 2 (c).

Step 2: If no Lidar points can be found in both boxes, the line segment is removed because the line segment is far from a building. If Lidar points are found in both boxes and the density values of the two boxes almost equal, the line segment is removed because the line segment surrounded by Lidar points should locate on the rooftops. The remaining line segments are considered as possible boundary segments. The following processes are to get the accurate boundary segments from the possible object segments.

Step 3: Grouping the remaining line segments. As the line segments are extracted with principal orientations constraint, the remaining line segments have two orientations and are grouped according to their angles and distances. Three parallel object segments in one group can be found in Figure 2 (c).

Step 4: Two rectangle boxes are also generated for each segment in Figure 2 (c). The difference in Lidar point density of the two boxes is calculated for each segment. The basic principle is that the difference in Lidar point density of an accurate boundary is larger than that of an inaccurate boundary. A data set of the difference in Lidar point density in a group is defined as formula 1.

$$L = \{ |d_k| \mid k = 0, \dots, m \} \quad (1)$$

d_k means the difference in Lidar point density of a segment. The Kmeans clustering algorithm with $K=2$ is applied to divide the data set into two sets, a set with big difference values and a set with small difference values. The segments with the data set of small difference values will be eliminated. The remaining line segments are identifies as the boundary segments. The selected boundary segment is demonstrated in Figure 2(d).

3. EVALUATION

3.1 Data set

In this study, both aerial stereo pairs and orthoimage can be used to test the effect of our approach. Comparing with an aerial image, an orthoimage can contain a much larger area and more buildings. So a true orthoimage are used to test the effect and applicability of our approach shown in Figure 3(a). The image is in a size of 7300*8300 pixels, which spatial resolution is 5cm. Lidar data in same area have average point spacing of 1.1m. The image contains a large area and more buildings with different orientations, different structures, and different texture conditions. As shown in Figure 3(a), the buildings have different orientations, and most of buildings have complex geometric shapes. Image texture conditions are also different, including simple texture, highly repeated texture, and complex texture. The complex texture conditions are formed because the trees are so close to the buildings.

3.2 Experimental results and discussion

The line segment extraction algorithm proposed in this study is an accurate and robust method for peak detection on accumulative space of Hough transformation. It is compared with a classical peak detection method based on maximum value, max-value method. Figure 3(b) and (c) are the results of line segments extraction by max-value method and our algorithm, respectively. The results show that the orientations of all segments in Figure 3(c) are almost coincided with the principle orientations of the building while segments in Figure 3(b) are not. It also shows that almost all important boundaries extracted by max-value method are extracted by our algorithm, but a few important boundaries extracted by our algorithm successfully are not obtained by the max-value method. It is shown in detail by label A, B in the rectangle box in Figure 3(c). Compared to the max-value method, our algorithm performs better in avoiding missing boundary details. The reason that more detailed boundary segments can be detected by our algorithm is that peak detection on accumulative space of Hough transformation with principal orientation constraint

become more robust, which makes the boundaries with weak signals in image can be robustly detected.

To demonstrate the effectiveness of the proposed algorithm for boundary segments selection, it is compared with the result of line segments extraction. Figure 3(d) are the results of boundary segments selected from Figure 3 (c). Comparing Figure 3(c) and (d), the number of line segments reduces from 4141 to 779, 3362 line segments (81%) have been removed by our selection algorithm. The final boundaries in Figure 3(d) are overlain with the original image, which shows that all important segments of building boundaries are kept; most of irrelative line segments (mainly line segments of the rooftops) have been removed. And the determined boundaries are detailed and have a highly geometric precision.

To evaluate the quality of the boundaries quantitatively, the correctness of the boundaries are estimated. We check the distance and angle between a boundary segment and its corresponding segment in the original image. If the angle is smaller than 3 degrees and the distance is smaller than 5 pixels, then the boundary segment is considered as a true one; otherwise, it is considered as a wrong one. There are 779 boundary segments in Figure 3(d), 709 true boundaries are found according to the evaluation criterion. To evaluate the quality of the boundaries quantitatively, the correctness of the boundaries are estimated. We check the distance and angle between a boundary segment and its corresponding segment in the original image. If the angle is smaller than 3 degrees and the distance is smaller than 5 pixels, then the boundary segment is considered as a true one; otherwise, it is considered as a wrong one. There are 779 boundary segments in Figure 3(d), 709 true boundaries are found according to the evaluation criterion. Only 70 boundaries are determined wrongly by our approach. The correctness of the determined boundaries is 91%. By overlapping the final boundaries, the original image, and Lidar data, it can be found that almost all wrong boundaries are kept wrongly because of a local jump of density of Lidar data, and most of the wrong boundaries lie in the rooftop of building.

4. CONCLUSIONS

To automatically obtain detailed building boundaries with precise geometric position, a new approach integrated very high resolution imagery and Lidar data is proposed in this study. The approach consists of a sequence of four steps: pre-processing, building image generation, line segments extraction, and boundary segments selection. Firstly, the segmented building points need to be determined from raw Lidar data. Then, a building image is generated by processing an original image using a bounding rectangle and a buffering zone, which are derived from the segmented building points. Based on the building image and rough principal orientations constraints, an algorithm is proposed for estimating the principal orientations of a building, which ensures the accuracy and robustness of the subsequent line segments extraction. Finally, an algorithm based on Lidar point density analysis and Kmeans clustering is proposed to identify accurate boundary segments from the extracted line segments dynamically. All these strategies ensure a high correctness (91%) of the determined boundaries. And the boundaries are detailed and have a highly geometric precision.

REFERENCES

Brenner, C., 2005. Building reconstruction from images and laser scanning. *International Journal of Applied Earth Observation and Geoinformation*, 6(3/4), pp. 187-198.

Chaudhuri, D. and Samal, A., 2007. A simple method for fitting of bounding rectangle to closed regions. *Pattern Recognition*, 40(7), pp. 1981-1989.

Haala, N. and Brenner, C., 1999. Virtual city models from laser altimeter and 2D map data. *Photogrammetric Engineering and Remote Sensing*, 65(79), pp. 787-795.

Kim, T. and Muller, J. P., 1999. Development of a graph-based approach for building detection. *Image and Vision Computing*, 17(1), pp. 3-14.

Kraus, K. and Pfeifer, N., 1998. Determination of terrain models in wooded areas with airborne laser scanner data. *ISPRS Journal of Photogrammetry and Remote Sensing*, 53(4), pp. 193-203.

Lin, C. and Nevatia, R., 1998. Building detection and description from a single intensity image. *Computer Vision Image Understanding*, 72(2), pp. 101-121.

Mayer, H., 1999. Automatic object extraction from aerial imagery - a survey focusing on buildings. *Computer Vision and Image Understanding*, 74(2), pp. 1

Mayer, S., 2001. Constrained optimization of building contours from high resolution ortho-images. In: *Proceedings of International Conference on Image Processing*. 38-149.

Rottensteiner, F., Trinder, J., Clode, S. and Kubik, K., 2005. Using the Dempster-Shafer method for the fusion of Lidar data and multi-spectral images for building detection. *Information Fusion*, 6(4), pp. 283-300.

Sampath, A. and Shan, J., 2007. Building boundary tracing and regularization from airborne Lidar point clouds. *Photogrammetric Engineering and Remote Sensing*, 73(7), pp. 805-812.

Sohn, G. and Dowman, I., 2004. Extraction of buildings from high resolution satellite data and LIDAR. In: *ISPRS 20th Congress WGIII/4*, Istanbul, Turkey.

Suveg, I. and Vosselman, G., 2004. Reconstruction of 3D building models from aerial images and maps. *ISPRS Journal of Photogrammetry and Remote Sensing*, 58(3/4), pp. 202-224.

Vosselman, G. and Kessels, P., 2005. The utilisation of airborne laser scanning for mapping. *International Journal of Applied Earth Observations and Geoinformation*, 6(3/4), pp. 177-186.

Weidner, U. and Forstner, W., 1995. Towards automatic building extraction from high resolution digital elevation models. *ISPRS Journal of Photogrammetry and Remote Sensing*, 50(4), pp. 38-49.

Rau, J. Y. and Chen, L. C., 2003. Fast straight lines detection using hough transform with principal axis analysis. *Journal of Photogrammetry and Remote Sensing*, 8(1), pp. 15-34.

Xu, F., Niu, X. and Li, R., 2002. Automatic recognition of civil infrastructure objects using hopfield neural networks. In: *ASPRS annual conference*.

Zhang, K., Yan, J. and Chen, S. C., 2006. Automatic construction of building footprints from airborne Lidar data. *IEEE Transaction on Geoscience and Remote Sensing*, 44(9), pp. 2523-2533.

ACKNOWLEDGEMENTS

This work was supported by 973 Project (Grant No. 2006CB701300) and the China / Ireland science and technology collaboration research fund (ICT, 2006-2007).

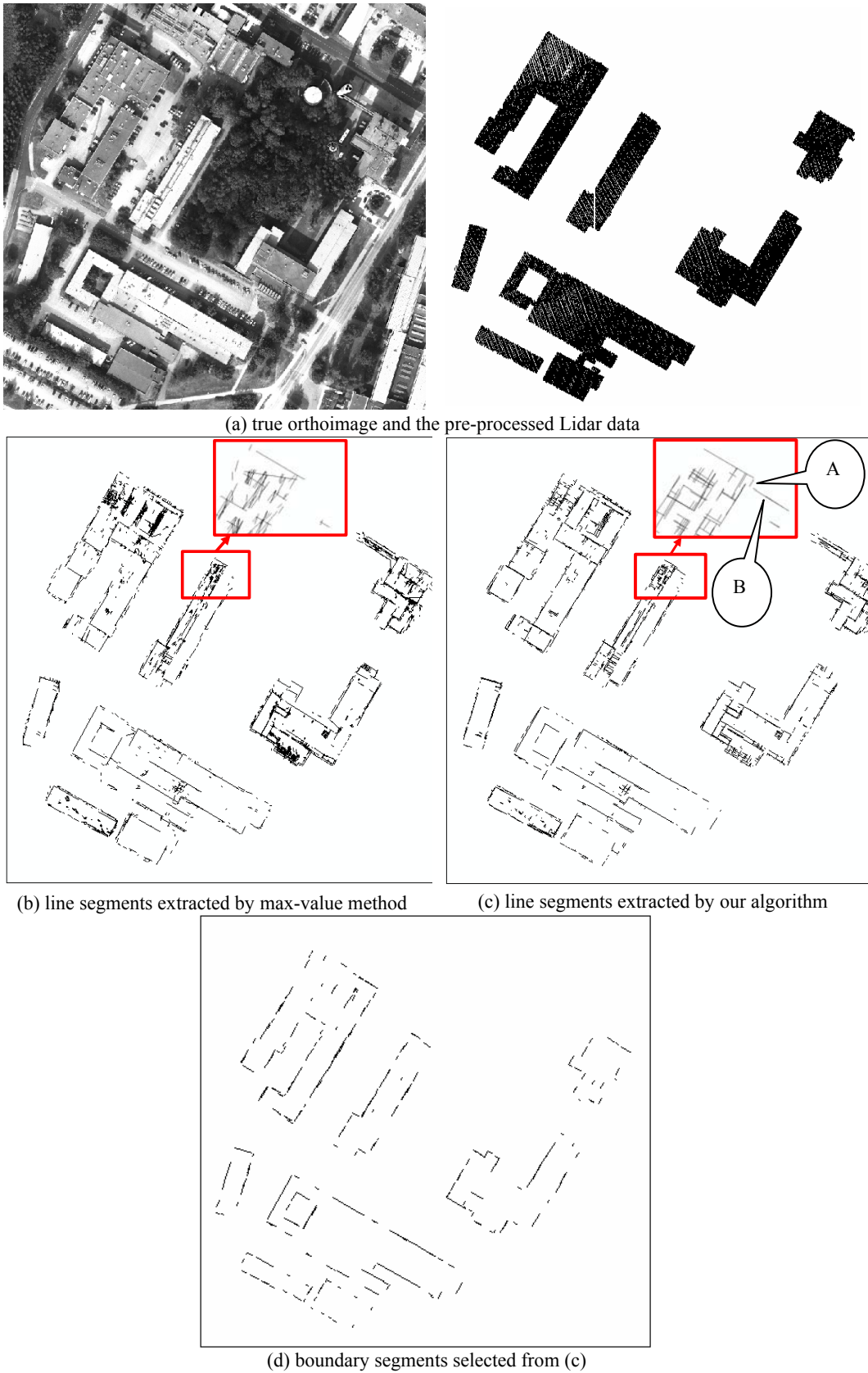


Figure 3. Building boundary determination by a high resolution image(5cm) and Lidar data